

USING BINARY PULSARS TO TEST LORENTZ SYMMETRY IN THE GRAVITATIONAL SECTOR

J.M. WEISBERG

*Department of Physics and Astronomy, Carleton College
Northfield, MN 55057, USA
E-mail: jweisber@carleton.edu*

I review some of the major developments in the theoretical background and experimental uses of binary pulsars to explore local Lorentz invariance in the gravitational sector and its possible violation.

1. Binary pulsars

A binary pulsar (PSR) consists of a spinning neutron star (NS) with a radio beam, and a companion, in a mutual orbit. The companion is usually another compact object — either another NS or a white dwarf (WD). A typical NS is a highly relativistic object. With mass $M \sim 1.4M_{\text{Sun}}$ and radius $R \sim 10$ km, the NS has $GM/(c^2R) \sim 0.2$. Furthermore, the PSR's radio pulses serve as a highly precise spin-powered clock, enabling the accurate measurement of the spin and orbital parameters of the binary system and the testing of relativistic gravitational effects in strong-field conditions. For example, the double NS system PSR B1913+16 has provided the first evidence for the existence of gravitational waves,¹ while NS-WD systems tend to be the best binary PSRs for probing violations of Lorentz invariance.

2. PPN extensions and PFE in binary PSRs

The weak-field, parametrized post-newtonian (PPN) framework was extended in Ref. 2 to include the possibility of preferred-frame effects (PFE), via parameters α_1 , α_2 , and α_3 . This analysis was further augmented to encompass the strong fields of binary PSRs,³ as follows.

A gravitational N -body post-newtonian lagrangian was derived with terms for $\hat{\alpha}_1$ and $\hat{\alpha}_2$, where the 'hat' over a parameter indicates that it is a strong-field modification of the PPN version; commensurate with the

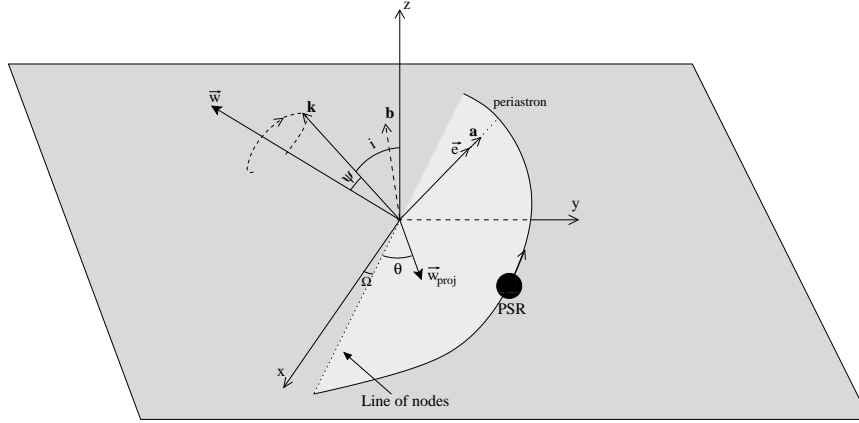


Fig. 1. PSR orbital geometry. Unit vectors $\{\mathbf{a}, \mathbf{b}, \mathbf{k}\}$ define an orthogonal coordinate system centered on the binary's center of mass, with \mathbf{a} and \mathbf{b} in the orbital plane (lightly shaded) and \mathbf{k} pointing in the direction of orbital angular momentum. Coordinate \mathbf{a} points toward PSR periastron, and $\mathbf{a} \times \mathbf{b} = \mathbf{k}$. The eccentricity e is incorporated into the vector $\vec{\mathbf{e}} = e \mathbf{a}$. The unit vectors $\{\mathbf{x}, \mathbf{y}, \mathbf{z}\}$ define another orthogonal coordinate system, with \mathbf{x} and \mathbf{y} in the plane of the sky (heavily shaded), and \mathbf{z} pointing *from* the observer *to* the binary's center of mass. Unit vector \mathbf{x} points toward celestial north. This right-handed coordinate system is opposite to the observers' convention for the plane of the sky. The velocity of the binary system's center of mass with respect to the preferred frame and its projection onto the orbital plane are $\vec{\mathbf{w}}$ and $\vec{\mathbf{w}}_{\text{proj}}$, respectively. Adapted from Ref. 4.

highly relativistic environment of a binary PSR system. The $\hat{\alpha}_1$ -part of the lagrangian includes a dependence of the vector velocity $\vec{\mathbf{w}}$ of the binary center of mass with respect to the preferred frame, leading to some potentially measurable effects. For small-eccentricity binary PSRs, the eccentricity vector $\vec{\mathbf{e}} \equiv e \mathbf{a}$ (see Fig. 1) undergoes the following time evolution:

$$\vec{\mathbf{e}}(t) = \vec{\mathbf{e}}_{\text{Rel}}(t) + \vec{\mathbf{e}}_{\text{Fixed}}; \quad (1)$$

where the first term results from the usual general relativistic advance of periastron whose mean rate is $\langle \dot{\omega}_{\text{Rel}} \rangle$; but the second is a nonzero constant 'polarizing' term resulting from PFE, and proportional to G_{orb} (a function of orbital parameters and component masses), $\hat{\alpha}_1$ and $\vec{\mathbf{w}}_{\text{proj}}$ (the projection of $\vec{\mathbf{w}}$ onto the orbital plane):

$$\vec{\mathbf{e}}_{\text{Fixed}} = G_{\text{orb}} \hat{\alpha}_1 \mathbf{k} \times \vec{\mathbf{w}}_{\text{proj}}, \quad (2)$$

(which points in the orbital plane, perpendicular to $\vec{\mathbf{w}}_{\text{proj}}$). Hence the measurement of eccentricity over time affords the possibility of separating the two terms in Eq. (1) and then, for a given choice of preferred frame of

\vec{w} (e.g., the cosmic microwave background), determining the desired PFE parameter $\hat{\alpha}_1$ from Eq. 2.

However, some observational difficulties remain. First, the velocity of the binary system's center of mass with respect to Earth is difficult to measure, which limits the accuracy of \vec{w} (both its direction and magnitude). Also the angle Ω is not measurable from PSR timing, thereby further limiting the accuracy of its projection \vec{w}_{proj} . In general, statistical arguments must be employed in order to ameliorate these limitations, although much progress has also been made in overcoming them observationally. (See below.) The measured eccentricity for the NS-WD PSR B1855+09 system was then combined with the above analysis to provide an upper limit on $|\hat{\alpha}_1|$ of 5.0×10^{-4} , which was comparable to contemporaneous solar system limits, and (unlike the solar system case) measured in *strong* gravitational fields.

Building upon the work of Ref. 3, it was shown⁴ that *both* $\hat{\alpha}_1$ and $\hat{\alpha}_2$ are determinable from timing measurements of low-eccentricity binary PSRs, and the new analysis was applied to two additional NS-WD binary PSR systems: PSR J1012+5307 and PSR J1738+0333, as follows.

A nonzero $\hat{\alpha}_2$ will cause precession of the orbital pole, \mathbf{k} , about \vec{w} (see Fig. 1). This precession leads to an observable consequence in the PSR timing measurable $x \equiv a_{\text{PSR}} \sin i$. Here a_{PSR} is the semimajor axis of the PSR orbit, and i is the 'inclination' angle between \mathbf{k} and \mathbf{z} :

$$\left(\frac{\dot{x}}{x}\right)_{\hat{\alpha}_2} = -\frac{\hat{\alpha}_2}{4} \left(\frac{2\pi}{P_b}\right) \left(\frac{w}{c}\right)^2 \cot i \sin 2\psi \cos \theta, \quad (3)$$

where angles ψ and θ specify the instantaneous direction of \vec{w} in the (precessing) $\{\mathbf{a}, \mathbf{b}, \mathbf{k}\}$ coordinate system, as shown in Fig. 1. However, there are observational difficulties in determining w and the angles, similar to those discussed above in the determination of $\hat{\alpha}_1$. While significant progress has been made, the nature of PSR timing observations prevents the determination of Ω and hence accurate values of w , θ , and ψ , so it remains necessary to use statistical arguments to extract the PFE parameter $\hat{\alpha}_2$. A joint analysis from both pulsars leads to $|\hat{\alpha}_2| < 1.8 \times 10^{-4}$. This limit is far weaker than the solar system limit of Ref. 5, but does have the benefit of probing strong fields. The analysis of $|\hat{\alpha}_1|$ of Ref. 3 was also revisited. With the benefit of additional kinds of observational data that leave only Ω undetermined, an upper limit on $\hat{\alpha}_1$ of $(-0.4 [+3.7, -3.1]) \times 10^{-5}$ was found for PSR J1738+0333, making it the best extant constraint for this parameter.

The determination of PPN parameter α_3 from binary PSRs was derived theoretically in Ref. 6; Ref. 7 reports an exquisitely precise null measurement, as expected in semiconservative theories of gravitation.

3. SME coefficients for Lorentz violation in binary PSRs

The first extensive theoretical SME analysis of the signal of Lorentz violation in binary PSRs was published in Ref. 8. In developing the general theory, twenty independent Lorentz-violating coefficients were found, including nine in the field $\bar{s}^{\mu\nu}$. It was shown that three of the PPN parameters are expressible in terms of the single coefficient \bar{s}^{00} ; and that $\alpha_1 = 4\alpha_2$, indicating that (at least in the weak-field limit), they are not independent. More importantly, it was shown that binary PSR secular *measurables* $\langle\dot{\omega}_{Rel}\rangle$, $\langle de/dt\rangle$, and $\langle di/dt\rangle$ can be expressed in terms of combinations of projections of the SME $\bar{s}^{\mu\nu}$ along the orbital axes $\{\mathbf{a}, \mathbf{b}, \mathbf{k}\}$, raising the prospect of determining these SME Lorentz-violating coefficients via binary PSR timing observations. Therefore wholly new tests of Lorentz violation become available which are not accessible in the PPN formulation.

4. Future prospects

Observationally, the most promising direction involves the detection and measurement of additional binary PSR systems. These would increase the parameter-space coverage of current tests, which could lead for example to disentangling the currently covariant SME Lorentz-violation coefficients,⁸ and increasing the sky coverage of Lorentz-violation tests.⁴ Planned new, highly sensitive radiotelescopes will detect numerous such systems.⁹ Theoretically, the most exciting prospect includes the generation of additional SME measurables in binary PSR systems.

Acknowledgments

This research was supported by NSF grant AST-0807556.

References

1. J.M. Weisberg, D.J. Nice, and J.H. Taylor, *Ap. J.* **722**, 1030 (2010).
2. C.M. Will and K. Nordtvedt Jr., *Ap. J.* **177**, 757 (1972).
3. T. Damour and G. Esposito-Farèse, *Phys. Rev. D* **46**, 4128 (1992).
4. L. Shao and N. Wex, *Class. Quantum Grav.* **29**, 215018 (2012).
5. K. Nordtvedt, *Ap. J.* **320**, 871 (1987).
6. J.F. Bell and T. Damour, *Class. Quantum Grav.* **13**, 3121 (1996).
7. M.E. Gonzalez *et al.*, *Ap. J.* **743**, 102 (2011).
8. Q.G. Bailey and V.A. Kostelecký, *Phys. Rev. D* **74**, 045001 (2006).
9. J.M. Cordes *et al.*, *New Astron. Rev.* **48**, 1413 (2004).